TUM-HEP xxxx/19

QCD phase transition in cosmology

Aldo Gamboa,[1*] **David Guzmán,**[1†] **Víctor Knapp**[1‡]
José Padua[1,2§] **and Saúl Ramos-Sánchez**[2,3¶]

[1] *Facultad de Ciencias, Universidad Nacional Autónoma de México, POB 70-542, Cd.Mx. 04510, México*

[2] *Instituto de Física, Universidad Nacional Autónoma de México, POB 20-364, Cd.Mx. 01000, México*

[3] *Physik Department T75, Technische Universität München, James-Franck-Straße 1, 85748 Garching, Germany*

Abstract

Nice abstract. Very nice indeed!!

[*] aldojavier@ciencias.unam.mx
[†] david_guzmanr@ciencias.unam.mx
[‡] victorknapp@ciencias.unam.mx
[§] jospadua@ciencias.unam.mx
[¶] ramos@fisica.unam.mx

1 Introduction

According to the ΛCDM model, most of the matter that shapes the Universe as we know it was created during the three minutes that followed the often called *big bang*, the beginning of time about 14 billion years ago. The whole observable Universe reduced originally to a point experienced suddenly a rapid and violent expansion, which concluded, when the Universe was barely 10^{-32} s old, with the appearance of particles and antiparticles in equal amounts, and light, distributed homogeneously in an already vast space. At a temperature as high as 10^{26} K in that epoch, due to their homogeneous distribution, the hot content of the Universe can be described as a thermal bath with the properties of a perfect fluid. As the volume of the Universe continued its growth, the pressure and temperature of the hot fluid were smoothly reduced.

About 10^{-10} s after the big bang, when the temperature had reduced to nearly 10^{15} K, it is thought that a series of conditions [1] allowed for a (tiny) imbalance between matter and antimatter that produced the matter domination that rules the Universe today. At the level of elementary particles physics, these conditions include that the rates at which matter and antimatter interact must differ, which happens (non-perturbatively) even in the Standard Model (SM). Another important condition is that this process must have occurred out of thermal equilibrium, so that it could not be reversed. In an expanding Universe, this naturally happens if the system experiences first order phase transitions, which are indeed likely to be part of the cosmological history.

It is believed that a cosmological phase transition between the quark-gluon plasma and hadron phases took place at $t \approx 10^{-5}$ s, which corresponds to a temperature of $T \sim 2 \times 10^{12}$ K. The theory that describes the dynamics of hadrons is called *Quantum Chromodynamics* QCD. In QCD the fundamental objects are the spin-1/2 fermions called *quarks* which carry a color charge[1] and the interactions are mediated through 8 massless bosons force carries called *gluons*. The main difference between QCD and electromagnetism is the fact that free quarks are not found in nature but joined in groups that make zero color charge such as baryons and mesons. Such phenomenon is called *confinement* and occurs because the coupling α_s between color-charged objects grows with distance in what is called *asymptotic freedom* [2], [3]. Nevertheless, at high energies or early times in the Universe, the strong force decreases and quarks and gluons can deconfine from the colorless objects and exist as free particles in a state named the *quark-gluon plasma* QGP. This deconfinement process might be a first-order phase transition in some scenarios [4].

If the QCD phase transition is of first order then, according to nucleation theory, it would have proceeded with the formation of bubbles of hadronic matter in the quark-gluon plasma. These bubbles continue to grow during the process and, near the end of the transition, the last shrinking regions would have been filled with a concentrated baryon number due to the difficulty for the baryons to diffuse through the phase boundary [5]. Therefore, the baryon density in the quark-gluon plasma is higher than in the hadron phase, giving a baryon density contrast.

In the high-density regions produced by the phase transition, the neutrons are diffused more than the protons because they do not interact electromagnetically with electrons. So there is not only inhomogeneities in the baryon number but in the neutron-to-proton ratios: the high-density regions have a lower neutron-to-proton ratio while the low-density regions have a higher neutron-to-proton ratio [6].

[1] Similar to the electromagnetic charge but with three different varieties named as red, green and blue.

Historically, one of the main interests in a first order QCD phase transition was the possibility to influence Big Bang Nucleosynthesis (BBN), the process in which the lightest elements, such as ^{4}He, D, ^{3}He and ^{7}Li, were produced in the early Universe (from 10 s to 20 min in the range of temperatures from 10^{10} K to 10^9 K). BBN is one of the main observational evidences for the ΛCDM model, the other ones being the Cosmic Microwave Background and the expansion of the Universe. The abundances of the lightest elements can be calculated with the Standard Big Bang Nucleosynthesis (SBBN) model, which has a single free parameter, the baryon-to-photon ratio η, and is based on the Standard Model physics alone.

The SBBN model is the simplest theoretical framework which is in good agreement with astrophysical observations. Nevertheless, it poses a fine-tuning problem: the predicted abundances can vary if the conditions or the physics at early times are changed. Also, this model has disagreements with other methods used to estimate the value of η [5]. The objective of nonstandard BBN models is to alleviate these problems. For instance, the Inhomogeneous Big Bang Nucleosynthesis model (IBBN) assumes the existence of regions with high and low baryon densities during the process of nucleosynthesis, consequently allowing η to be a function of position, and adding the separation of the high-density regions as another parameter for the model.

The model of IBBN naturally fits as a consequence of a first order QCD phase transition because the latter allows the existence of regions with inhomogeneities. Nevertheless, the minimal requirement for this scenario is that the mean bubble nucleation distance has to be greater than the proton diffusion length ($\sim$ 3 m at the time of QCD transition) [7]. As it will be seen in this paper, the required value for the mean distance between inhomogeneities is not achieved.

Recently the interest in a possible QCD first order phase transition have been reborn due to the discovery of gravitational waves [8]. Cosmological first order phase transitions could have produced gravitational waves due to the collisions of the bubbles made during the transition. The generated power spectrum could depend on the bubble radius and on the time that the transition lasted [9].

Although current knowledge of cosmology indicates that the most probable scenario is that the QCD phase transition was a crossover [10], some people propose that, due to our current ignorance of the early history of the Universe, a QCD first order phase transition could have happened. For example, according to [11], if three or more light quarks were present during the QCD phase transition, a first order phase transition would have happened producing black holes already detected by LIGO/VIRGO detectors. Other scenarios where a QCD first order phase transition is realized can be seen in [12] and [13].

This paper is organized as follows. In section 2, we present some basic notions of cosmology needed to understand the framework in which we are working; in section 3, we discuss the phenomena of phase transitions emphasizing in first order phase transitions, and then, in section 4, we relate this discussion to the QCD phase transition and we talk about the collective properties of the QGP plasma and the hadron gas. In section 5, we review some aspects of nucleation theory necessary to compute the nucleation rate of bubbles for the QCD phase transition scenario and we present the most important parameters needed to understand the general behavior of the generated bubbles. In section 6, we present the theoretical framework used to describe the growth and expansion of the nucleated bubbles in a radiation-dominated flat Universe, arriving to a system of integro-differential equations. In section 7, we present and discuss the results obtained for the evolution of the bubbles during the QCD phase transition, and finally, in section 8 we give the conclusions and suggestions for future work. In this paper, we are going to work with natural units, so that $c = k_B = \hbar = 1$.

2 Some Standard Cosmology Basics

Modern cosmology studies the properties of the universe as a whole at scales of the order of few 100 Mpc, with the aim of understanding its origin and evolution. It tries to solve fundamental questions, such as the predominance of matter over antimatter, the origin of the chemical elements and how the structures in the Universe were made, just to name a few.

The standard cosmological model is based on the *cosmological principle*, which states that the Universe is homogeneous and isotropic, and on the assumption that our physical models are valid at all times throughout the Universe. The theory of General Relativity is used to describe the dynamics of the Universe. We need a metric $g_{\mu\nu}$, which describes the geometry of the Universe, and an energy-momentum tensor $T_{\mu\nu}$ representing its physical content, together with the Einstein field equations:

$$R_{\mu\nu} - \frac{1}{2} R\, g_{\mu\nu} = 8\pi G\; T_{\mu\nu}, \tag{1}$$

where $R_{\mu\nu}$ and R are respectively the Ricci tensor and Ricci scalar and G is Newton's gravitational constant.

It can be proven that the cosmological principle is satisfied by the Friedmann-Lemaître-Robertson-Walker (FLRW) metric $g_{\mu\nu}$, associated with the space-time interval:

$$ds^2 = g_{\mu\nu}\, dx^\mu dx^\nu = dt^2 - a(t)^2 \left(\frac{dr^2}{1 - k\, r^2} + r^2\, d\theta^2 + r^2 \sin^2\theta\, d\phi^2 \right), \tag{2}$$

where r, θ and ϕ are the usual spherical coordinates, t is the *cosmic time*, $a(t)$ is the *scale factor* and k is a constant representing the curvature of space. These coordinates are known as *comoving coordinates* and do not change with the expansion of the Universe. In a *comoving frame* the matter of the Universe which only moves with the expansion, is at rest, so it can be defined a *comoving volume* which remains constant with the expansion. In this volume the number densities of objects in rest with respect to the comoving frame, remain constant.

For $k = 0$ we have a spatially-flat Universe (Euclidean space), for $k = 1$ we have a positively curved Universe (elliptical space) and for $k = -1$ we have a negatively curved Universe (hyperbolic space).

The assumptions of homogeneity and isotropy also set strong constraints on the energy-momentum tensor [14], which has to take the form of that of an ideal gas:

$$T_{\mu\nu} = [\epsilon(t) + P(t)] U_\mu U_\nu + P(t)\, g_{\mu\nu}\,, \tag{3}$$

where $\epsilon(t)$ is the energy density, $P(t)$ is the pressure of the fluid and U_μ is the four-velocity of the fluid, which can have more than one component or *species*. If these components are non-interacting, then we will have that $\epsilon(t) = \sum \epsilon_i(t)$ and $P(t) = \sum P_i(t)$.

The dynamics of the Universe can be established with the three equations above. The results are the *Friedmann equations*:

$$H^2 + \frac{k}{a^2} = \frac{8\pi G}{3}\epsilon\,, \tag{4a}$$

$$\frac{\ddot{a}}{a} = -\frac{4\pi G}{3}\left(\epsilon + 3P\right)\,, \tag{4b}$$

where $H = \dot{a}/a$ is the *Hubble parameter*. Rewriting eq. (4a) we get:

$$\frac{k}{a^2 H^2} = \frac{8\pi G}{3H^2}\epsilon - 1 \equiv \frac{\epsilon}{\epsilon_c} - 1, \tag{5}$$

where $\epsilon_c = 3H^2/8\pi G$ is the *critical density* and tell us the value of ϵ and time at which the Universe is flat, $k = 0$. Currently, observations suggest a flat Universe since the value of the energy density is close to the critical value [15]. Since the flatness of the Universe depends so precisely in the value of the energy density, it is hard to believe that a perfect balance between a closed and an open Universe prevailed during the evolution of the Universe. This is known as the *flatness problem*. To solve this and other problems in the ΛCDM model, the latter is extended with the *cosmological inflation* which is a theoretical epoch of an incredibly fast expansion of the Universe. Inflation theory predicts that the fast growth of the Universe would have expanded away any large-scale curvature, giving $k = 0$, thus solving the flatness problem.

Combining equations (4a) and (4b), or equivalently, using the more general relation $T^{\mu\nu}{}_{;\nu} = 0$, we obtain:

$$\frac{d\epsilon}{dt} = -3\,\frac{1}{a}\frac{da}{dt}\,(\epsilon + P)\,, \tag{6}$$

which establishes the dynamics of ϵ and P for energy conservation in the Universe. Nevertheless, there are three variables (a, ϵ, P) for just two independent equations. To complete the system, an *equation of state* is introduced, which relates the energy density with the pressure of each component of the fluid through the relation:

$$P_i(t) = w_i\,\epsilon_i(t), \tag{7}$$

where w_i is a value that depends on the nature of the component of the fluid. Cosmological observations suggest the existence of three principal components of the Universe: relativistic particles, non-relativistic particles and dark energy.

The energy density of each of the components in the Universe have a different dependence with the scale factor, determined by eqs. (6) and (7). For non-relativistic particles, we have $w = 0$, because the pressure is much smaller than the energy density, so eq. (6) gives us $\epsilon \propto a^{-3}$, which represents the dilution of volume densities due to the cosmic expansion. For relativistic particles, the energy density is dominated by the kinetic energy, giving a radiation-like behavior for which it is well known that the pressure and radiation are related by $P = \frac{1}{3}\epsilon$, so eq. (6) implies $\epsilon \propto a^{-4}$. This relation takes into account the cosmic expansion and the redshifting of the energy. Finally, for dark energy we have $P = -\epsilon$, giving us a constant energy density, according to (6). It can be seen that this particular choice of w for dark energy leads to an accelerated expansion of the Universe. Summarizing

$$w = \begin{cases} 0 & \text{non-relativistic particles} \\ \frac{1}{3} & \text{relativistic particles} \\ -1 & \text{dark energy} \end{cases} \qquad \text{and} \qquad \epsilon = \begin{cases} a^{-3} & \text{non-relativistic particles} \\ a^{-4} & \text{relativistic particles} \\ \text{const.} & \text{dark energy} \end{cases} \tag{8}$$

The dependence in time of the scale factor implies that the energy densities are themselves functions of time. Nevertheless, they can be related to the temperature of the Universe using some basic results from statistical physics.

In an ideal collection of particles, the ensemble-averaged properties of the system can be described by a one-particle distribution function f, which can be related to the number density of particles by integrating f over the momentum. For a quantum mechanical system, the distribution function takes the form [16]:

$$f(p) = \frac{1}{e^{\frac{E(p)-\mu}{T}} \pm 1}\,, \tag{9}$$

where $E(p) = \sqrt{p^2 + m^2}$ is the energy of a relativistic particle with momentum p and mass m, μ is the chemical potential and T is the temperature of the system. The positive sign is for a system of fermions (Fermi-Dirac distribution) and the negative sign is for a system of bosons (Bose-Einstein distribution).

For a radiation dominated Universe, i.e. one filled with relativistic particles, we can use the distribution function (9) to calculate the energy density [17]:

$$\epsilon = \frac{g}{(2\pi)^3} \int d^3p \, f(p) E(p), \tag{10}$$

where g represents the number of degrees of freedom of the particles in the system.

Physically, the chemical potential represents the released or absorbed energy of the system when the number of particles in the system change. As will be seen later, we are interested in the case where the chemical potential is approximately zero. In that case and taking into account that for relativistic particles $m \ll T$, we get from eq. (10):

$$\epsilon(T) = \frac{\pi^2}{30} \, g \, T^4 \times \begin{cases} 1 & \text{for bosons} \\ \frac{7}{8} & \text{for fermions} \end{cases} \tag{11}$$

which establishes the explicit relation between the energy density for relativistic particles and the temperature. Furthermore, from eqs. (8) and (11), we get $T \propto a^{-1}$ for relativistic particles, so an expanding Universe implies a diminution of temperature with time.

At early times, all the existent particles were relativistic. As the temperature dropped, the number of different particles in equilibrium decreased and a series of events took place, constituting the thermal history of the Universe. Among these events are the QCD phase transition and the Big Bang Nucleosynthesis.

3 Phase Transitions and Thermodynamics

Boiling water or making ice in a fridge may be a everyday phenomena, but they bear similarities with more exotic ones like superconductivity, superfluidity and the subject of this work. The common aspect between them is that they undergo a *phase transition*, *i.e.* a drastic change of the properties of a thermodynamic system. Formally, this drastic change is in a non-analyticity (divergencies or discontinuities in the derivatives) in the free energy of the system. The modern classification of phase transitions dictates that when there is a latent heat[2] in the phase transition it is called a *first order phase transition*, otherwise we called them a *second order phase transition*.

All the thermodynamic quantities of a system are encoded in the internal energy $U(S, V, N_i)$. The extensive variables, like the volume, entropy and particle number, of the system can be obtained by extremizing $U(S, V, N_i)$ while the intensive variables, like the temperature, pressure and chemical potential, are the partial derivatives of $U(S, V, N_i)$. From a physical perspective, U can be interpreted as the work required to *create* the system. Sometimes there is a constraint on our system, in which case it is convenient to use U's Legendre transformations, also known as thermodynamic potentials. For example, if temperature is fixed, it is useful to use the Helmholtz free energy $F(T, V, N_i) := U - TS$ instead of U. Now the values taken by V and N_i are those that extremize F at a given T. In this case F is to be interpreted as the work required to create the system on an environment of temperature T. Landau developed

[2] Amount of heat released or supplied during the phase transition.

a formalism to study phase transitions where the free energy also depends on a new variable called the *order parameter* o, so that $F = F(T, V, N_i; o)$. The order parameter is a quantity that changes accordingly to the phase in which the system is. It is generally chosen that it is zero during a phase and different from zero in the other phase. For example, in the liquid-gas phase transition the order parameter is the difference of densities $o = \rho - \rho_{gas}$. An extra equilibrium condition is then added in order to extremize F, namely: $\frac{\partial F}{\partial o} \stackrel{!}{=} 0$. The solutions to this equation may correspond to different phases and their respective Helmoltz free energies F_* are obtained by the evaluations $F(T, V, N_i, o_*)$ with the corresponding o_*.

Furthermore, the change in the order parameter is different depending on the type of phase transition. Physically, the existence of a latent heat implies that while this heat is being supplied or released during the phase transition the system is in a mixture of the two phases. Therefore, in a first order phase transition the order parameter suffers a discontinuous jump. For example, when boiling water from a liquid phase, the order parameter starts with an order parameter $o \neq 0$ at the beginning of the phase transition but when the transition ends and all the water is now vapor, then $o = 0$. For a second order phase transition the order parameter changes continuously.

The latent heat L can always be written as

$$L = T\Delta S = V\Delta\omega, \tag{12}$$

where ΔS is the change of the entropy from one phase to another, V is the volume and ΔH is the change in the entalphy density $\omega = \epsilon + p$. From equation (12), we can see that the non-analiticity in the free energy is reflected in the first derivative of the free energy which is the entropy $S = \frac{\partial F}{\partial T}$.

Another type of changes in the matter are the so called *crossovers*. In Figure 1(a), we show a schematic of the phase diagram of the liquid-gas phase transition of water. The dot is called the critical point (CP). The transition from liquid to gas happens as a first order phase transition along the transition line which is the continuous line in the Figure 1(a). In the CP, the phase transition is of second order. For temperatures higher than the critical temperature T_c and pressures higher than P_c there is not a real phase transition because the non-analiticities in the free energy vanish. Thus, water in these conditions is neither liquid nor gas but a different state of matter that effuses through solids like a gas and dissolves like liquid [18]. Nevertheless, there is a continuation to the transition line called the Widom line which is depicted as the dotted line in Figure 1(a). In [19] it was shown that when crossing the Widom line, argon fluid presented a drastic change in sound dispersion[3]. Thus, the behaviour of the fluid changed drastically when crossing the Widom line although it is not a real phase transition.

In Figure 1(b) it is presented the heat capacity and the density during a isobaric first order liquid-gas phase transition in oxygen at constant pressure of $4\,Mpa$ and the same curves for a crossover through the Widom line at $10\,Mpa$. In the $4Mpa$ there is the expected divergence in the heat capacity that happens during a first liquid-gas phase transition with the corresponding discontinuous jump in the density which is the order parameter. For the crossover transition the heat capacity exhibits a maximum instead of an infinity. At the same temperature the density has an inflection point which corresponds to a maximum in the derivative of the density respect to the temperature. The (pseudo)critical temperatare of the crossover is then fixed as the temperarure at which this two things happen.

[3]The change in speed of an acoustic wave depending on its wavelength

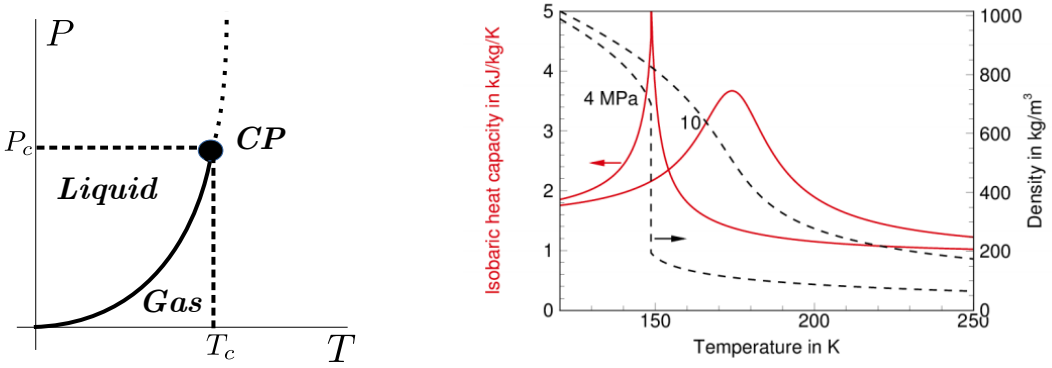

(a) (b)

Figure 1: (a)Phase diagram of water. The Continuous line representes the first order phase transition coexistence line. The big dot is the critical point at which water exhibits a second order phase transition. The dotted line is the Widom line corresponding to the crossover transition. [20] (b) The density and the heat capacity as a function of the temperature during a first order phase transition at constant pressure $P = 4Mpa$ and during a crossover transition at constant $10MPa$ in oxygen. Figure from [21] with data from [22].

4 The QCD Phase Transition

According to our discussion in the Introduction, the quarks that made up baryons and mesons can deconfine at high energies, or equivalently high temperatures or high chemical potentials. The deconfinement process can be analyzed through an order parameter as seen in Section 3. In this case, the order parameter is the thermal average of the trace of the Polyakov Loop [23]. Currently, very large computer programs are made to simulate QCD in what is known as Lattice QCD. They look when and how the parameter orders change to establish the character of the QCD phase transitions. For zero dynamical quarks $N_f = 0$[4] and baryonic chemical potential $\mu_B = 0$ the confinement transition is of first order. Nevertheless, when introducing two dynamical quarks $N_f = 2$ the transition becomes a crossover as discussed in Figure 1.When using Lattice QCD, it is customary to define the (pseudo)critical temperature as the temperature where the derivative of the order parameter with respect to the temperature has a maximum. The range of the pseudo-critical temperatures reported in the literature goes from $150 - 200$ MeV [23] [24]. Unfortunately, for large μ_B Lattice QCD fails to give a critical or pseudocritical temperature.

Several studies have predicted that for large baryon chemical potential $\mu_B \sim 1\,GeV$ with $\mu_B = \mu_q$ where μ_q is the quark chemical potential, then the transition could be a first order [25]. The point where the transition line changes from being a crossover to a first order is called the *critical end point* (CEP). The chemical potential at which the confinement/deconfinement transition occurs for zero temperature is expected to be around 1 GeV. Roughly speaking, the mass of most baryons are around $1\,GeV$ and when the chemical potential surpasses this energy, the baryons start to penetrate each other changing the hadronic to quark-like degrees of freedom.

Other transitions are present in the QCD Phase Diagram. For example, the liquid-gas phase transition at low temperatures which is typically a first order phase transition but ends

[4] A dynamical quark have a mass much smaller than the energy scale of the system, in this case the temperature

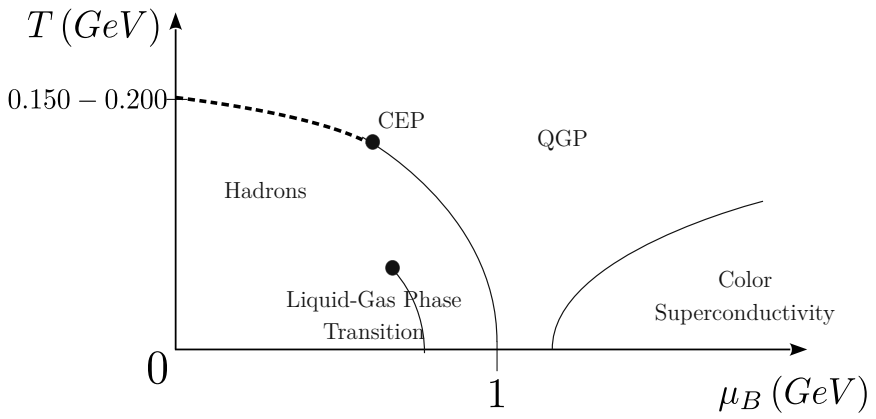

Figure 2: The conjectured QCD phase diagram for $N_f = 2$ dynamical quarks. The dotted line denotes the pseudocritical temperature for the crossover in the deconfinement transition. The point where the transition changes from a crossover to a first order is called the critical end point (CEP). The solid line after the CEP is the first-order transition line for the deconfinement. It is also shown the first-order phase transition line for the liquid-gas nuclear phase transition which ends in a second order-phase transition. At the right side of the diagram it is shown the transition line that separates the color-superconductor phase. Image adapted from [26].

up being a second-order phase transition in the last point of the transition line. Another more exotic quark state of matter has been conjectured named as color superconductivity where quarks join to form Cooper-like pairs through a phase transition [23]. The last paragraphs are summarized in Figure 2.

As seen in Figure 2, for $\mu_B \sim 0$ the transition is most likely a crossover. Because of the measured value of the baryon to photon ratio $\eta \sim 10^{-10}$ we know that in the Universe the chemical potential[5] was about $\mu_B \sim 0$. Nevertheless, the transition could have been first order if the number of dynamical quarks was $N_f \geq 3$ [4], this could have happened, for example, if the mass of the quarks was suppressed by some mechanism as in [11] leading to an increment of the dynamical quarks. There could also have been a very early first order phase transition, if by some mechanism the baryonic chemical potential $\mu_B \sim T$ as stated in [13]. Furthermore, another possibility stated in [12] says that a very early QCD first order phase transition could have been possible if the coupling constant of QCD is modified. In this work, we are going to stay with the asssumption that $\mu_B = 0$.

In order to get the evolution of a cosmological QCD phase transition we need to know the densities and pressures of the confined and deconfined phases. Let us consider the QGP and the hadron gas as ideal relativistic fluids, so that $P = \frac{1}{3}\epsilon$. Then, according to eq. (11):

$$\epsilon = \frac{\pi^2}{30}T^4 \times \begin{cases} g_{QGP}, & \text{QGP .} \\ g_h, & \text{hadron gas.} \end{cases} \quad \text{and} \quad P = \frac{\pi^2}{90}T^4 \times \begin{cases} g_{QGP}, & \text{QGP.} \\ g_h, & \text{hadron gas.} \end{cases}, \tag{13}$$

where $g_{QGP} = \frac{7}{8}g_{QGP,f} + g_{QGP,b}$ and $g_{QGP,f}$ are the fermionic degrees of freedom for the QGP, and $g_{QGP,b}$ the bosonic degrees of freedom for the QGP. Similarly g_h for the hadron gas phase. Let us determine both g's.

In both phases we have photons, neutrinos, electrons and muons which have a lower mass than the QCD phase transition temperature (the critical temperature will be discussed in

[5]The baryonic chemical potential can be interpreted as the asymmetry between baryons and antibaryons

Section 5 but it will be at least of $T_c = 200$ MeV). This number of degrees of freedom for both phases is

$$g_{both} = \frac{7}{8}\left(\underbrace{6}_{neutrinos} + \underbrace{4}_{electrons} + \underbrace{4}_{muons}\right) + \underbrace{2}_{photons} = 14.25, \tag{14}$$

where we have counted the spin, the particle/antiparticle possibilities, and the fact that there are only three left-handed neutrinos in the standard model, according to current limits [27].

According to current results [4], in order to have a first order phase transition there must be $N_f \geq 3$ quarks. Thus, in the case of the quark gluon-plasma, there are N_f quarks and 8 massless gluons. So we have

$$g_{QGP} = \frac{7}{8}\underbrace{(N_f \times 3 \times 2 \times 2)}_{quarks} + \underbrace{(8 \times 2)}_{gluons} + g_{both} = 10.5N_f + 16 + 14.25 = 10.5N_f + 30.25, \tag{15}$$

where we have counted the possible spin, the particle/antiparticle degrees of freedom, the color variations for the quarks and the two possible polarizations of the gluons.

For the hadronic state we count only three pions[6] which are the only relativistic hadrons below the critical temperature. So,

$$g_h = \underbrace{3}_{pions} + g_{both} = 17.25 \tag{16}$$

One final ingredient for the ϵ's and P's is missing. The main difference between the QGP and the hadronic phases is the fact that quarks are confined in hadrons. One way to account for this is adding a negative pressure B (or bag constant) to the QGP pressure P_{QGP} that reflects the fact that hadrons are stopped from being free by an inward pressure; and sum the same bag constant B to the energy density ϵ_{QGP} to account for the fact that we now have confined states in the hadronic phase. This is known as the MIT Bag Model. Therefore,

$$\epsilon = \begin{cases} \frac{\pi^2}{30}T^4(10.5N_f + 30.25) + B, & \text{QGP.} \\ \frac{\pi^2}{30}T^4(17.25), & \text{hadron gas.} \end{cases} \quad \text{and} \quad P = \begin{cases} \frac{\pi^2}{90}T^4(10.5N_f + 30.25) - B, & \text{QGP.} \\ \frac{\pi^2}{90}T^4(17.25), & \text{hadron gas.} \end{cases}, \tag{17}$$

where we require that $B = \frac{\pi^2}{90}g_q\left(1 - \frac{g_h}{g_q}\right)T_c^4$. This condition is imposed in order to fulfill the requirement that when the transition begins at $T = T_c$ the pressures have to be $P_h = P_q$.

5 Nucleation Theory

Everyday boiling water, or in every first order phase transition, dictates that when we rise the temperature of liquid water until its critical temperature, the liquid will transform to water vapor while staying in a constant temperature. Nevertheless, this is not always the case. When liquid water achieves high levels of purity, there are no external agents and there is an absence of walls, then it can be *superheated* to a temperature higher than the critical one without evaporating the water (or *supercooled* if the transition goes from vapor to liquid water). As the temperature rises above the critical one, bubbles of vapour will appear within the water but will fail to expand until a certain temperature is achieved. At this temperature, the bubbles are nucleated with a *critical radius* which is the necessary radius for a bubble to

[6] With masses of 139 MeV for the charged pions [28] and 135 MeV [29]

grow instead of shrink. After this, the bubbles with critical radius begin to grow until the system is filled with water vapor. If the appearance of bubbles is caused by some remaining impurities, the process is called *heterogeneous nucleation*. If there is no impurity present in the system, it is called *homogeneous nucleation*. The main goal of nucleation theory is to compute the probability of forming a bubble of critical radius r_* per unit time per unit volume. This process corresponds to classical nucleation, nevertheless the QCD Phase transition is a relativistic quantum nucleation. Furthermore, it was a homogeneous nucleation because it was the first QCD phase transition ever made and there were no impurities.

To have a rough idea of what relativistic quantum nucleation theory is, consider a quantum field ϕ and the potential $U(\phi)$ shown in Figure 3(a). $U(\phi)$ has two degenerate minima, ϕ_L and ϕ_H. For $T > T_c$ the minimum ϕ_H corresponds to the high temperature phase because it is the least energy configuration. The other minimum ϕ_L is the vacuum corresponding to the low temperature phase.

Due to the tunnelling effect, it is clear that the field can go from ϕ_L to ϕ_H. A trick is done to calculate the probability from the field to go from ϕ_L to ϕ_H with the semiclassical (WKB) approximation. Although the WKB approximation cannot be applied to the potential shown in Figure 3(a) due to the non-existence of a classical solution to this path, the transformation $t \to -i\tau$, where τ is called the *euclidean time*, is defined and inverts the normal potential as in Figure 3(a) to the one in Figure 3(b). Then, in Euclidean time, there exists a classical path from ϕ_H to ϕ_L. According to the WKB approximation the probability of going from ϕ_H to ϕ_L goes like $\sim e^{-S_E}$, where S_E is the action in euclidean time evaluated in the euclidean classical allowed path. Thus, the nucleation rate in relativistic quantum theory goes like $\sim e^{-S_E}$. This theory of relativistic nucleation was developed in [30] and [31].

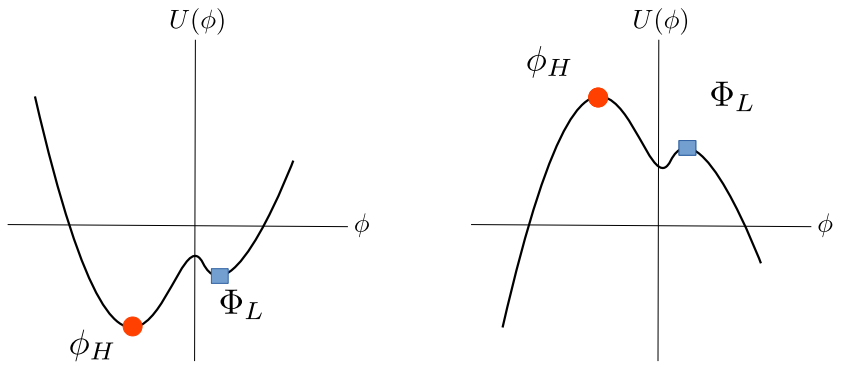

Figure 3: (a) Potential for the quantum field ϕ which has two minima ϕ_H and ϕ_L which correspond to the high temperature and low temperature phases respectively. (b) Potential for the quantum field ϕ in Euclidean time.

Evaluating the relativistic-quantum expression for the nucleation rate due to its complexity is, in general, done numerically. As pointed out in the last section, the QGP can be treated as a relativistic fluid; under this assumption the nucleation rate was evaluated by Csernai and Kapusta [32] using relativistic hydrodynamics and classical nucleation theory. Classically, the nucleation rate may be expected to be proportional to a Boltzmann distribution-like function $e^{-\frac{F}{T}}$ ($k_B = 1$) because the nucleation rate is the probability of going from one configuration to another one in a thermodynamic system which can be studied as a canonical ensemble. This

was deduced from first principles by Langer [33] and established that

$$I = \frac{\Omega}{2\pi}\kappa e^{-\frac{\Delta F}{T}}, \tag{18}$$

where Ω is called the statistical prefactor which accounts for the available phase space as the system goes from one phase to another, κ is called the dynamical prefactor which accounts for the growth of the bubble and ΔF is the change of free energy of the system from going to one phase to the other. For the QCD phase transition scenario, the probability of nucleating a bubble of the L-phase out of the H-phase, evaluated by Csernai and Kapusta [32], is

$$I = \frac{1}{2\pi}\underbrace{2\left(\frac{\sigma}{3T}\right)^{3/2}\left(\frac{r_*}{\xi_H}\right)^4}_{\Omega}\underbrace{\frac{4\sigma(\zeta_H + 4\eta_H/3)}{(\Delta\omega)^2 r_*^3}}_{\kappa} e^{-\Delta F_*/T} = \frac{4}{\pi}\left(\frac{\sigma}{3T}\right)^{3/2}\frac{\sigma(3\zeta_H + 4\eta_H)r_*}{3(\Delta\omega)^2\xi_H^4}e^{-\Delta F_*/T}, \tag{19}$$

where σ is the surface tension of the bubbles, T is the temperature, ζ_H is the bulk viscosity of the H-phase, η_H is the shear viscosity of the H phase, $\Delta\omega$ is the difference of enthalpy density $\omega = P + \epsilon$ between the phases, which can be interpreted as the latent heat per volume, and ξ_H a correlation length to be defined below. Note that this nucleation rate refers to the phase transition from H to L. If one wants the probability of nucleating an H-phase bubble out of the L-phase, then the subscripts have to be changed $H \leftrightarrow L$ in (19).

To completely evaluate (19) we need to know ΔF, η_H, ζ_H, ξ_H and σ. The free energy difference ΔF will be evaluated in the next section. The two viscosities ζ_H and η_H are, generally, related to the difficulty of the fluid to be compressed and deformed respectively. As shown in [34], for a QCD coupling constant α_s between 0 and 0.3, $\zeta \ll \eta$ which physically implies that the quark gluon-plasma is much easily deformed than compressed. According to Csernai and Kapusta [32], $\alpha_s = 0.23$ near $T_c = 200$ MeV. Thus, we can neglect ζ_H in (19). The shear viscosity according to [35] and [36] has the general form $\eta_H = CT^3$ with C a constant determined by the number of dynamical quarks and the value of the coupling constant. For two dynamical quarks, $\eta_H = 18T^3$ according to Kapusta [37]. Nevertheless, the final average bubble radius depends very weakly in the value of C. Thus, we will take $\eta_H = 18T^3$ for all the scenarios considered in Section 7.

The surface tension of the bubbles σ has only been evaluated using Lattice QCD with no dynamical quarks in [38] [39] [40]. Nevertheless, to our knowledge there is not a value for a non-zero value of dynamical quarks. Csernai and Kapusta used the value of $\sigma = 50$ Mev/fm^2, but different values had been considered ranging from $\sigma = 50$ Mev/fm^2 to $\sigma = 450$ Mev/fm^2 [41]. In this work we will use three values $\sigma = 50, 150, 200$ Mev/fm^2 to analyze the dependence of the final average bubble radius with the surface tension.

The correlation length ξ_H defined in [32] depends on the barrier between the two phases as in Figure 3. This barrier can be associated with the bubble thickness and has to do with the energy necessary to go from phase to the other. According to Csernai and Kapusta, near the critical temperature ~ 200 MeV its value is $0.7\,fm$. Similar to the value of C in η_H, the final average bubble radius depends very weakly with ξ_H. Therefore, we will use $\xi_H = 0.7$ fm.

Finally, due to the different range of critical temperature for which the transition can occur at $\mu_B \sim 0$, we will analyze the final average bubble radius for $T_c = 160, 180, 200$ MeV.

6 Nucleation of hadrons in the early Universe.

As stated in Section 5, the QCD phase transition is modeled through homogeneous nucleation theory with hadronic *spherical* bubbles forming in the QGP. The first step to do so is to identify an order parameter. The order parameter must have a discontinuous behaviour at the critical temperature. As it will be seen later, the mean radius of the bubbles is zero for $T > T_c$, but for $T < T_c$ there is a discontinuous jump from zero to a non-vanishing value. Therefore the mean radius of the bubbles is the order parameter.

Now we must construct Landau's free energy functional F for a bubble in terms of its radius r, *i.e.* the energy required to create a bubble of radius r with environment temperature T. We begin by considering the surface tension σ of a bubble, defined as the ratio of the work W to the bubble's surface change ΔA due to W, *i.e.* σ is a proportionality factor such that the work W required to expand a bubble by ΔA is simply $\sigma \Delta A$. Therefore, the work required to *create* a bubble under our conditions has the contribution σS, with S the bubble's surface area.

The interior and exterior of the bubbles correspond to different phases, so in principle there may be a difference of pressure at the surface of the bubble. This tells us that to nucleate a bubble of volume V, one must oppose the external pressure and there is a work contribution of the form $V\Delta P = V(P_{ext} - P_{int}) = V(P_q - P_h)$, where we have used that the exterior phase is the QGP and the interior is the hadronic phase.

The total work required to create a bubble is then,

$$W = \sigma S + V\left(P_q - P_h\right)$$

and therefore, for a bubble of radius r,

$$F = 4\pi r^2 \sigma + \frac{4\pi}{3} r^3 (P_q - P_h)\,.$$

By applying the equilibrium condition $\frac{\partial F}{\partial r} = 0$ (as discussed in Section 3) we find that the critical radius at which bubbles nucleate is given by

$$r_* = \frac{2\sigma}{P_h - P_q}, \tag{20}$$

which we recognize as Laplace's equation and has a corresponding Helmholtz free energy of the form

$$F_* = \frac{4\pi}{3} \sigma r_*^2\,. \tag{21}$$

Because $P_{int}(T_c) = P_{ext}(T_c)$ it follows that r_* changes discontinuously when passing through T_c, which is consistent with this being a first order phase transition.

F_* is the thermodynamic potential that contains the information we are interested in. It will allow us to study how the hadronic and QGP volumes compare and evolve. The hadronic and QGP volumes, denoted by V_h and V_q respectively, are quantified by the fraction $h(t)$ which has the form $h(t) = \frac{V_h(t)}{\Omega(t)}$, where $\Omega(t)$ is the total volume. From now on, we shall work on the comoving frame, so that Ω is constant. Additionally, h codifies the average bubble radius $\bar{r}$ *via*

$$\frac{4\pi}{3} \bar{r}(t)^3 n(t) = h(t), \tag{22}$$

with n the number density of bubbles.

We shall now derive an expression for the hadronic volume $V_h(t)$ that will automatically provide us with one for $h(t)$ itself. Because the critical radius of a bubble depends in the difference of the phase pressures as seen in (20), then the critical radius depends on time. Thus, the size of a bubble depends on the time of creation t' and the time t which accounts for the growing of the bubble. So, we have a function of the form $V(t,t')$ which considers the initial volume $V(t',t')$ and the expansion from t' to t.

In order to compute the hadronic volume $V_h(t)$, we need to add the contributions of each bubble with size $V(t,t')$. Therefore, we need the number of bubbles nucleated. This is where the nucleation rate comes into play, because it quantifies how many bubbles are successfully nucleated per unit time per unit volume, which implies that the number of bubbles of critical sized formed in a time dt' in the available space $V_q(t')$[7] is $dt'I(t')V_q(t')$. Using that the QGP volume is $V_q = (1-h(t'))\Omega$ and adding the contributions of all the bubbles nucleated we get that the hadronic volume is

$$h(t)\Omega := V_h(t) = \int_{t_c}^{t} dt' I(t') V_q(t') V(t,t') = \int_{t_c}^{t} dt' I(t')(1-h(t'))\Omega V(t,t')\,, \tag{23}$$

where t_c is the critical time at which the transition occurs. Since Ω is constant, we have

$$h(t) \;=\; \int_{t_c}^{t} dt' I(t')(1-h(t'))V(t,t'). \tag{24}$$

Eq. (24) is an integral equation for $h(t)$ that, when coupled to the cosmological evolution of the Universe, provides the aspects of the QCD phase transition that we are interested in. However, before doing the coupling, we need an explicit expression for $V(t,t')$, which can be obtained by rewriting V as

$$V(t,t') = \frac{4}{3}\pi(r(t') + \Delta r(t,t'))^3 = \frac{4}{3}\pi\left(r_*(t') + \Delta r(t,t')\right)^3,$$

so that $\Delta r(t,t')$ accounts for the expansion of the bubble; we are no taking into account the growth of the bubbles due to the expansion of the Universe because, as we said earlier, we are working in the comoving frame. Therefore, if $v(t'')$ is the speed of the expanding surface of the bubble, then $\Delta r\,(t') = \int_{t'}^{t} dt'' v(t'')$. Thus,

$$V(t,t') = \frac{4}{3}\pi\left(r_*\left(t'\right) + \int_{t'}^{t} dt'' v\left(t''\right)\right)^3 \tag{25}$$

Furthermore, the bubble interface speed growth $v(t)$ was computed numerically by Miller and Pantano [42]. The computation was made using relativistic hydrodynamics with the equations of state given by (17). Thus, one expects that the dependence of the speed with time is realized through the temperature. Then, the speed is given by

$$v(T(t)) = 3\left(1 - \frac{T(t)}{T_c}\right)^{3/2}. \tag{26}$$

To compute $\bar{r}$ from equation (22), we must also know the expression for the number density of nucleated bubbles at time t, $n(t)$. First, we can derive an expression for the total number of particles $N(t)$ similarly to that of $h(t)$. As previously discussed, the number of bubbles

[7]The available space is $V_q(t')$ because bubbles cannot be created in the space that has already been transformed to the hadronic phase.

produced in a time dt' is $dt' I(t')(1-h(t'))\Omega$. Furthermore, one may think that computing the number density $n(t)$ would only need to consider the hadronic volume $V_h(t)$, *i.e.* $n(t) = \frac{N(t)(t)}{V_h(t)}$. However, the information we require from $n(t)$ is the average number of particles given an arbitrary portion of space or volume (see Figure 4). This is because we want to track down how the bubbles are occupying the whole space as the transitions evolves. Thus,

$$n(t) = \frac{N(t)}{\Omega} = \int_{t_c}^{t} dt' I(t')(1-h(t'))\,. \tag{27}$$

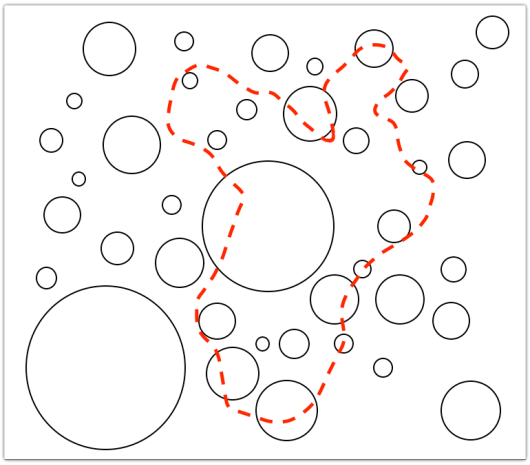

Figure 4: Cartoon of the phase transition. The number density must be obtained using the total volume Ω, as this allows us to know the average number of bubbles on an arbitrary sub-region (red).

Hitherto we have not coupled the time dependence of $h(t)$ to the dynamics of space-time, this can be achieved by using equations (4a) and (6). First we note that equation (6) implies that

$$\frac{d\epsilon}{da} = -\frac{3\omega}{a}\,. \tag{28}$$

Note that unlike the $\Delta\omega$ on (19), ω is the enthalpy density of the hole system and the analogous is true for ϵ. Given the extensive nature of energy and enthalpy, they must be given by the sum of their parts (hadrons and QGP) weighted by their respective volume fraction, so their densities satisfy,

$$\begin{aligned} \epsilon(t) &= h(t)\epsilon_h(t) + (1-h(t))\epsilon_q(t) \\ \omega(t) &= h(t)\omega_h(t) + (1-h(t))\omega_q(t). \end{aligned} \tag{29}$$

Equation (28) couples our model to a through (29). However, due to the time integration on (24) it is still necessary to relate a with t. This is precisely what equation (4a) does.

As discussed in section 2, the k on equation (4a) relates to the curvature of spacetime. Because this transition happened after inflation, we can consider k to be zero and therefore equation (4a) reduces to:

$$\frac{\dot{a}}{a} = \sqrt{\frac{8\pi}{3}\epsilon}\,. \tag{30}$$

Eqs. (24) and (28) define a system of integro-differential equations that determine the cosmological evolution of the phase transition where the dependant variables are the scale

factor h and T which depend on the scale factor $a(t)$. After solving for h and T we can compute the bubble number density through (27) and the average bubble radius with (22). We will now proceed to arrange the equations in a numerical-friendly way.

First, we have to rewrite equation (24) in terms of the scale factor $a(t)$. Using equation (30) to get the Jacobian, then

$$h(a) = \int_{a_c}^{a} da' \frac{1}{a'} \sqrt{\frac{3}{8\pi G\epsilon(a')}}\, I(T(a'))(1-h(a'))V(a,a'), \tag{31}$$

where the nucleation rate is given by equation (19) and the volume $V(t,t')$ given by equation (25). The nucleation rate depends on the the values $\sigma = 50, 150, 200\, Mev/fm^2$, $\eta = 18T^3$, $\zeta = 0$, $\xi = 0.7\, fm$, the critical radius given by equation (20), the equilibrium Helmholtz free energy given by (21), and the enthalpy difference $\Delta\omega = \omega_q - \omega_h$. The enthalpies given by $\omega_i = \epsilon_i + P_i$, for $i = q, h$, can be calculated through equations in (17).

For equation (30), we must solve for $\frac{dT}{dR}$. For this we plug equations (29) with (17) into equation (30), which gives

$$\frac{dT}{da} = -\frac{\frac{3w(a)}{a} + \frac{dh}{da}\left[\epsilon_h(T(a)) + \epsilon_q(T(a))\right]}{h(a)\frac{d\epsilon_h}{dT} + (1-h(a))\frac{d\epsilon_q}{dT}}. \tag{32}$$

.

Thus, the system of equations to solve are (31) and (32).

7 Results

In Fig. 5 we plot the evolution of the temperature, the nucleation rate, the bubble density, the average bubble radius, the energy and enthalpy densities, and the hadron fraction, with respect to the scale factor (which, in turn, is related to time through Friedmann equations) for different values for the surface tension, namely $\sigma = 50$, 150 and 200 MeV/fm^2. As discussed before, the value of σ for a non-zero value of dynamical quarks is not already known. So, we choose a set of values used in previous works.
We can see in Fig. 5(a) an identical behaviour like in [37]. The first part consists in a decrease in temperature due to the cosmic expansion. The temperature arrives at values lesser than the critical temperature, indicating the presence of a supercooling effect. Afterwards, there is a rise in temperature (known as reheating) due to the release of latent heat, as can be seen comparing Fig. 5(a) with Fig. 5(f). The enthalpy in Figure 5(f) is negative by definition. At first, it increases reaching a maximum and then having an abrupt decrease meaning this latent heat has been released. The release of latent heat comes from the energy lost by the quarks as they confine and indicates that this phase transition is exothermic. After that, the temperature continues increasing less rapidly. Before explaining what happens during this stage of lesser increase in the temperature, we can further clarify the nucleation of bubbles. In Fig. 5(c) we see the effective appearance of bubbles of critical size radius and in Fig. 5(d) we can see a discontinuous growth of the average radius, both occurring during the reheating. In Figure 5(d) the discontinuous jump during reheating is characteristic of a first order phase transition. This jump is also observed in Figure 5(c) where the number density jumps from zero to a finite value meaning that all bubbles are nucleated during the reheating. Then, the same number of bubbles nucleated begin to grow during the phase of lesser increase in the temperature, and no more are created since the nucleation rate vanishes as seen in Figure 5(b). After the reheating, in the stage of a less rapid increase in the temperature, the nucleated bubbles begin to occupy

the space, as can be seen in Fig. 5(g), until the hadron fraction is equal to one, meaning there is no QGP left in the comoving volume. Then, the transition is completed and the equations used for this analysis are no more valid.

The surface tension changes the magnitude of the nucleation rate I and the time at which happens. A greater surface tension means it is needed more energy to nucleate a bubble. Since the initial energy density is the same for the three cases as seen in Fig. 5(e), then, lesser bubbles are going to be nucleated for a greater surface tension, and these are going to be nucleated later because it is needed a greater supercooling to overcome the energy used to create the bubbles. Despite this, there is no change in the continuous decrease of the energy density due to the cosmic expansion as seen in Fig. 5(e). The value of the surface tension does not affect the energy because it only depends on the type of fluids considered and the temperature as seen in equation (11). The behaviour observed in Figure 5(e) is consistent with being a relativistic fluid. Furthermore, we can see that for smaller average radius in Fig. 5(d), the bubble number density has to be higher in order to reach $h = 1$ in the same amount of time.

As a next case, we consider the evolution of the same dynamical quantities in Fig. 6 for different values for the critical temperature, namely $T_c = 160$, 180 and 200 MeV. The plots of N, I, $\Delta\omega$ have their peaks at the same moment as in Figure 6(a) and behave similarly to Fig. 5. This means that for an earlier peak in the temperature, the nucleation rate is bigger and the number density is higher. We can see that the peak at which the bubbles start to nucleate happen before for higher critical temperatures. This is because for higher critical temperature the energy density is higher, as seen in Figure 6(c), therefore, because the surface energy is fixed the amount of energy necessary to start creating bubbles will be fulfilled before with higher energy density. From eq. (26) and Fig. 6(a) we can see that a greater critical temperature implies a lower speed of the expansion of the bubbles. This means that more bubbles are going to be nucleated in the same comoving volume because there is going to be more space without bubbles during the reheating phase (when the nucleation rate value is non-zero). The above reasoning is pictured in Fig. 6(b), where we see bubbles with a smaller average radius for greater critical temperatures which implies a bigger number density. Furthermore, the bubble radius increases with lesser critical temperature but not significantly as seen in Figure 6(b) and the duration of the transition is the same for all three critical temperatures as seen in Fig. 6(d).

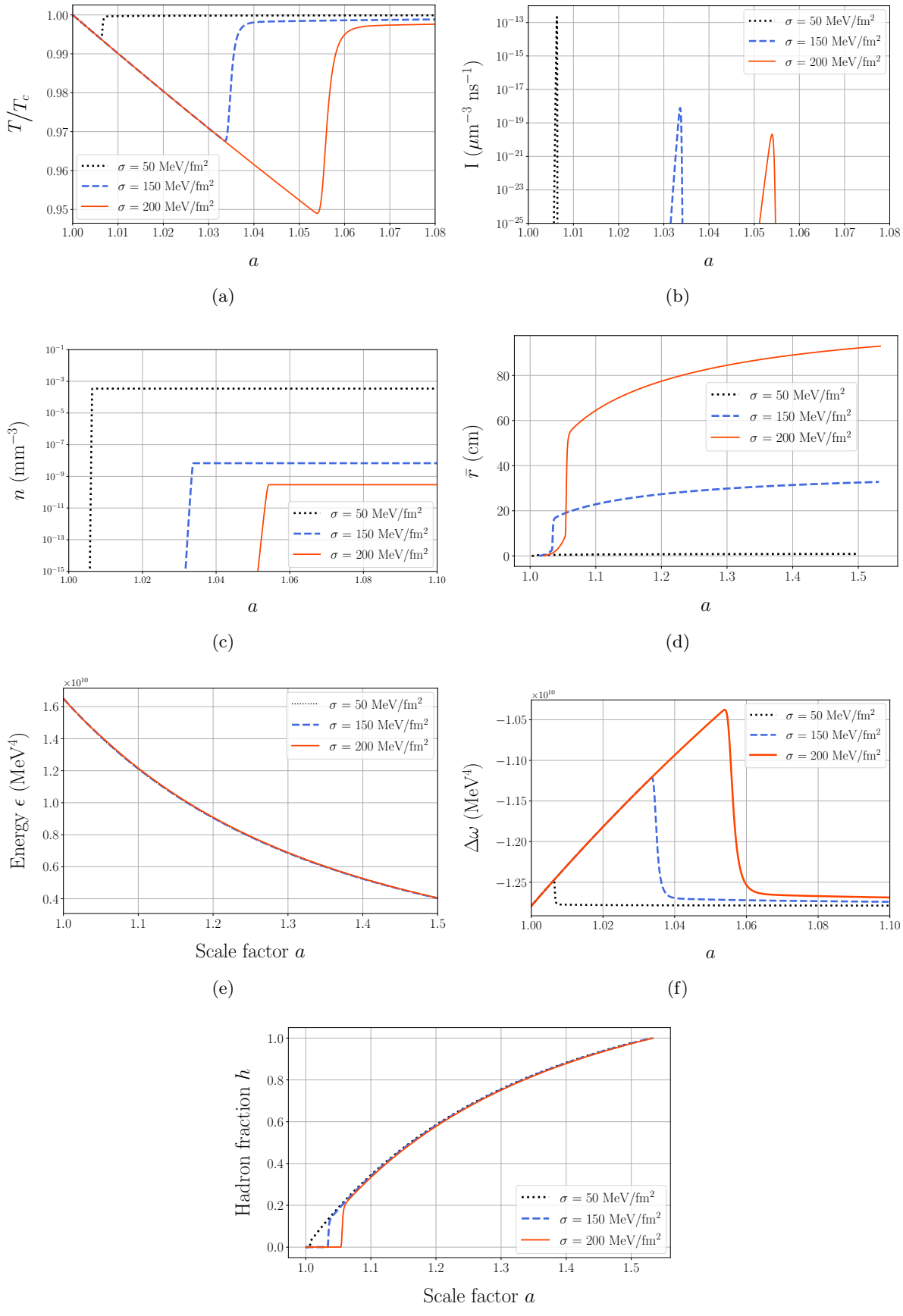

Figure 5: Evolution with respect to the scale factor of (a) temperature, (b) nucleation rate, (c) bubble density, (d) average bubble radius (the black dotted curves is non zero but much less than the other curves), (e) energy density, (f) enthalpy density and (g) hadron fraction for $\eta = 18T^3$, $\xi = 0.7$ fm, $\zeta = 0$, $g_h = 17.25$, $T_c = 160$ MeV and $g_q = 61.75$ (38 quarks).

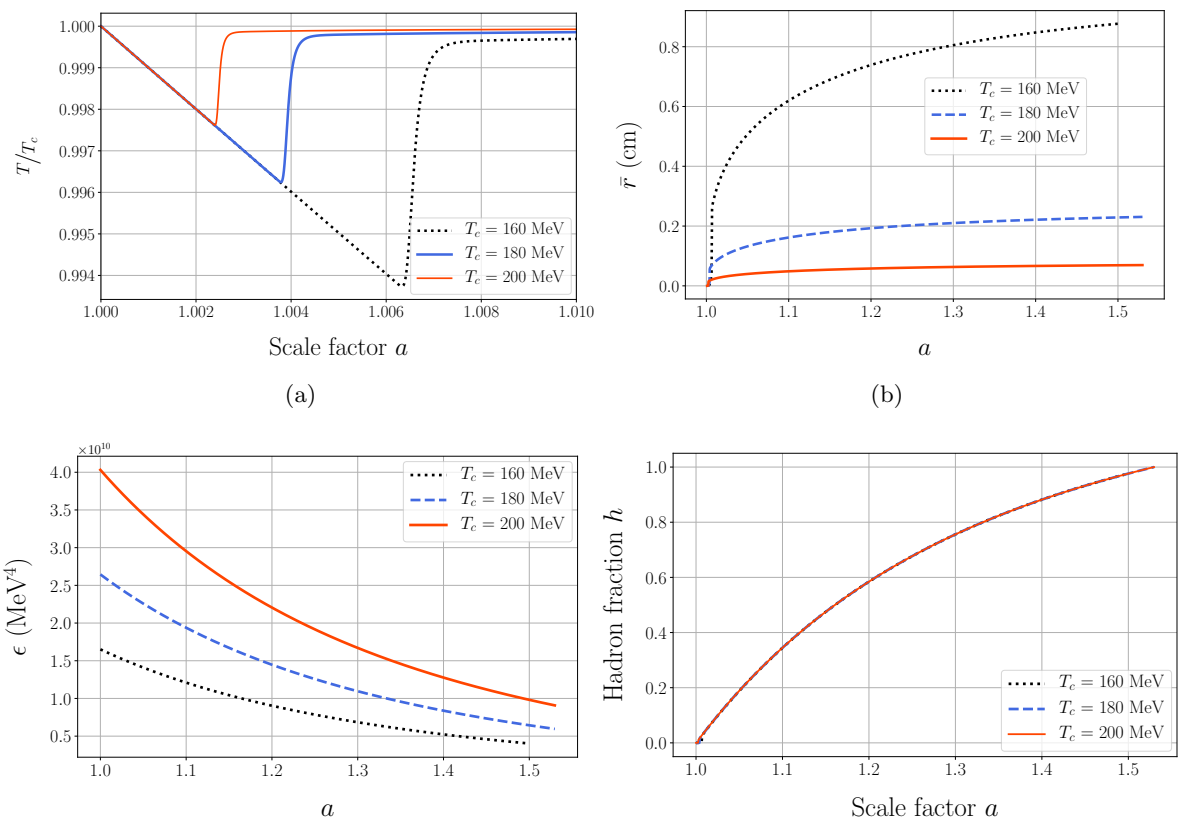

(a) (b) (c) (d)

Figure 6: Evolution with respect to the scale factor of (a) temperature, (b) average bubble radius, (c) energy density and (d) hadron fraction for $\eta = 18T^3$, $\xi = 0.7$ fm, $\zeta = 0$, $g_h = 17.25$ and $g_q = 61.75$ (3 quarks).

Finally, we studied the evolution bubbles for a different number of quarks and we plot the results in Fig. 7. From equation (11) we see that the energy density must be higher with more quarks. This is depicted in Fig. 7(c), but in all cases the energy density decreases which is consistent with the whole fluid being relativistic matter. Because for higher number of quark the energy density is higher, then the creation of bubbles happens before as seen in the peak of Fig. 7(a). The bubble radius changes but not significantly as seen in Fig. 7(b). Nevertheless, there is a change in the duration of the transition as seen in Fig. 7(d).

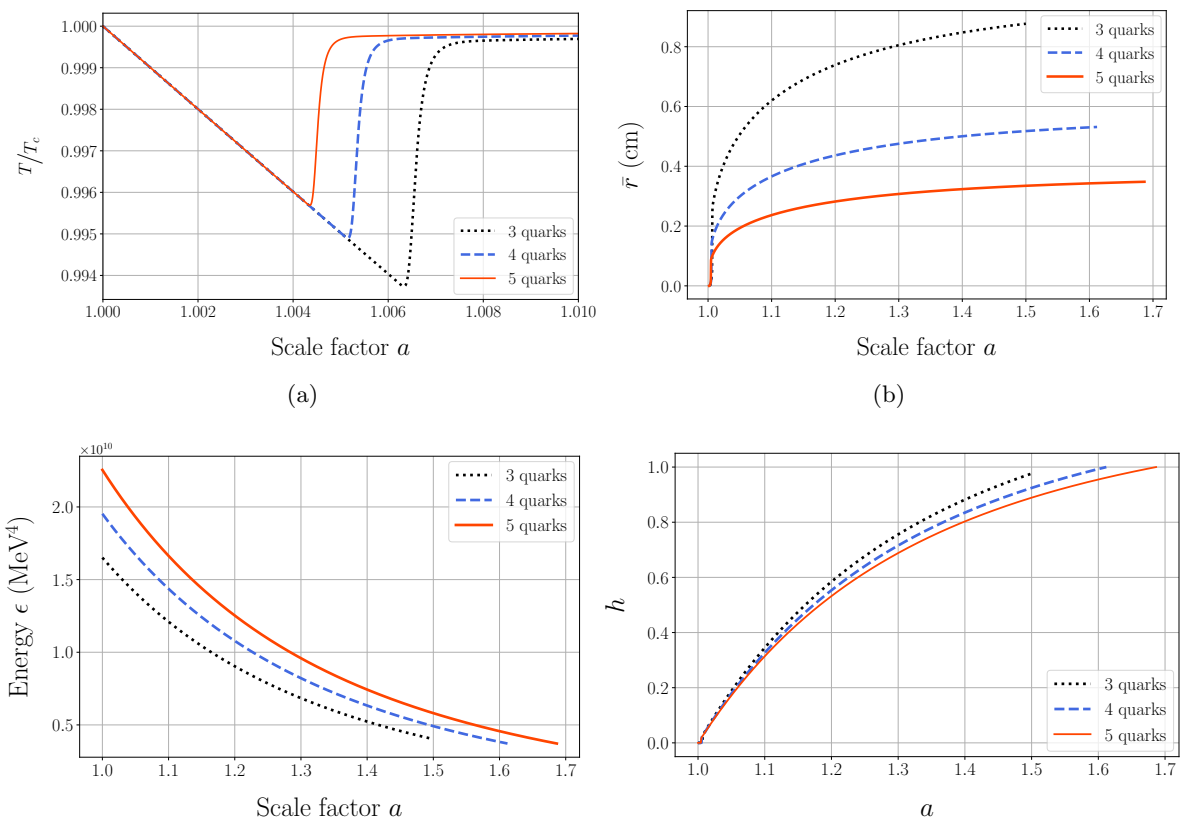

Figure 7: Evolution with respect to the scale factor of (a) temperature, (b) average bubble radius, (c) energy density and (d) hadron fraction for $\eta = 18T^3$, $\xi = 0.7$ fm, $\zeta = 0$, $g_h = 17.25$, $T_c = 160$ MeV.

8 Final remarks and outlook

We have introduced basic concepts in order to understand the evolution of a comoslogical QCD deconfinement first order phase transition using the MIT bag model. In Section 2 we introduced some basic concepts of standard cosmology. In Section 3 we review basic aspects of phase transitions emphasizing in first order phase transitions and explain the concept of crossover. In Section 4, we explain the conjectured QCD Phase diagram and mention the conditions in which the phase transition proceeded as first order and the equation of state of the QGP and the hadron gas in the MIT bag model. In Section 5 we introduce basic conceptos of nucleation theory and give an intuitive idea of the nucleation rate of hadronic bubbles in a QGP. Then, in section 6 we finally use the concepts previously introduced in order to establish the set of integro-differential equations which must be solved numerically. Finally, in Section 7 we discuss and analyze the behaviour of the transition varying the surface tension $\sigma = 50, 150, 200\, MeV$, the critical temperature $T_c = 160, 180, 200\, MeV$ and the number of dynamical quarks $N_f = 3, 4, 5$ quarks.

The general description of the evolution of the bubbles during the QCD first order phase transition is as follows: the cosmic expansion causes a decrease in the temperature of the Universe and reduces the interaction between the existent particles. The QGP does not transforms to the hadron gas at the critical temperature because of the purity of the universe. The QGP supercools below the critical temperature, because it needs energy to overcome the expense of

forming the surface of the hadron bubbles. At a certain point, the probability to nucleate a bubble begins to grow. The nucleation of bubbles releases latent heat to the thermal bath, thus reheating the Universe until the temperature is near its critical value; the energy released by the bubbles comes from the energy lost by the quarks as they are confined into hadrons. After that, both phases coexist at the same pressure and the hadronic bubbles continue their grow, releasing enough energy to increase the temperature. The transition ends when all the QGP has been converted into hadrons. Later, the cosmic expansion will decrease the temperature, continuing the thermal history of the Universe.

The contents of this article will hopefully be useful for a graduate or advanced graduate student who is pursuing starting to study a cosmological QCD phase transition. As stated in the introduction, the applications of a QCD first order phase transition include the influence on nucleosynthesis and the production of gravitational waves. Furthermore, the model can be extended adding a chemical potential as in [43]. This article may be the starting point in a project involving one of these.

Acknowledgments. It is a pleasure to thank ... This work was partly supported by DGAPA-PAPIIT grant IN100217 and CONACyT grants F-252167 and 278017.

References

[1] A. D. Sakharov, Pisma Zh. Eksp. Teor. Fiz. **5** (1967), 32, [Usp. Fiz. Nauk161,no.5,61(1991)].

[2] D. J. Gross and F. Wilczek, Phys. Rev. Lett. **30** (1973), 1343, [,271(1973)].

[3] H. D. Politzer, Phys. Rev. Lett. **30** (1973), 1346, [,274(1973)].

[4] M. D'Elia, Nucl. Phys. **A982** (2019), 99, arXiv:1809.10660 [hep-lat].

[5] H. Kurki-Suonio, Space Sci. Rev. **100** (2002), 249, arXiv:astro-ph/0112182 [astro-ph].

[6] H. Kurki-Suonio, R. A. Matzner, K. A. Olive, and D. N. Schramm, Astrophys. J. **353** (1990), 406.

[7] D. J. Schwarz, Annalen Phys. **12** (2003), 220, arXiv:astro-ph/0303574 [astro-ph].

[8] LIGO Scientific, Virgo, B. P. Abbott et al., Phys. Rev. Lett. **116** (2016), no. 6, 061102, arXiv:1602.03837 [gr-qc].

[9] C. Caprini, *Gravitational waves from cosmological phase transitions*, in *Proceedings, 45th Rencontres de Moriond on Cosmology: La Thuile, Italy, March 13-20, 2010*, 2010, pp. 257–264.

[10] Y. Aoki, G. Endrodi, Z. Fodor, S. D. Katz, and K. K. Szabo, Nature **443** (2006), 675, arXiv:hep-lat/0611014 [hep-lat].

[11] H. Davoudiasl, Phys. Rev. Lett. **123** (2019), no. 10, 101102, arXiv:1902.07805 [hep-ph].

[12] D. Croon, J. N. Howard, S. Ipek, and T. M. P. Tait, arXiv:1911.01432 [hep-ph].

[13] S. Schettler, T. Boeckel, and J. Schaffner-Bielich, Phys. Rev. **D83** (2011), 064030, arXiv:1010.4857 [astro-ph.CO].

[14] S. Weinberg, *Gravitation and Cosmology*, John Wiley and Sons, New York, 1972.

[15] Planck, N. Aghanim et al., arXiv:1807.06209 [astro-ph.CO].

[16] W. Greiner, L. Neise, and H. Stöcker, *Thermodynamics and statistical mechanics*, Classical theoretical physics, Springer-Verlag, 1995.

[17] D. Baumann, *Cosmology*, Lecture notes, 2019.

[18] H. J. J. Cleaves, Supercritical Fluid, 1, Springer Berlin Heidelberg, Berlin, Heidelberg, 2014, pp. 1–1.

[19] G. Simeoni, T. Bryk, F. Gorelli, M. Krisch, G. Ruocco, M. Santoro, and T. Scopigno, Nature Physics **6** (2010), 503.

[20] F. Maxim, C. Contescu, P. Boillat, B. Niceno, K. Karalis, A. Testino, and C. Ludwig, Nature Communications **10** (2019), 1.

[21] D. Banuti, M. Raju, and M. Ihme, Supercritical pseudoboiling for general fluids and its application to injection., 211, 01 2016, pp. 211–221.

[22] P. Linstrom, *Nist chemistry webbook, nist standard reference database 69*, 1997.

[23] K. Fukushima and T. Hatsuda, arXiv:1005.4814 [hep-ph].

[24] A. Ayala, arXiv:1608.04378 [hep-ph].

[25] A. Bender, G. I. Poulis, C. D. Roberts, S. M. Schmidt, and A. W. Thomas, Phys. Lett. **B431** (1998), 263, arXiv:nucl-th/9710069 [nucl-th].

[26] M. A. Stephanov, PoS **LAT2006** (2006), 024, arXiv:hep-lat/0701002 [hep-lat].

[27] ALEPH, DELPHI, L3, OPAL, SLD, LEP Electroweak Working Group, SLD Electroweak Group, SLD Heavy Flavour Group, S. Schael et al., Phys. Rept. **427** (2006), 257, arXiv:hep-ex/0509008 [hep-ex].

[28] M. Trassinelli et al., Phys. Lett. **B759** (2016), 583, arXiv:1605.03300 [physics.atom-ph].

[29] J. F. Crawford, M. Daum, R. Frosch, B. Jost, P. R. Kettle, R. M. Marshall, B. K. Wright, and K. O. H. Ziock, Phys. Rev. **D43** (1991), 46.

[30] I. Affleck, Phys. Rev. Lett. **46** (1981), 388.

[31] I. Affleck, Phys. Rev. Lett. **46** (1981), 388.

[32] L. P. Csernai and J. I. Kapusta, Phys. Rev. **D46** (1992), 1379.

[33] J. S. Langer, Annals Phys. **54** (1969), 258.

[34] P. Arnold, . Doan, and G. D. Moore, Physical Review D **74** (2006), no. 8.

[35] G. Baym, H. Monien, C. J. Pethick, and D. G. Ravenhall, Phys. Rev. Lett. **64** (1990), 1867.

[36] P. Arnold, G. D. Moore, and L. G. Yaffe, Journal of High Energy Physics **2003** (2003), no. 05, 051051.

[37] J. I. Kapusta and C. Gale, *Finite-temperature field theory: Principles and applications*, Cambridge Monographs on Mathematical Physics, Cambridge University Press, 2011.

[38] K. Kajantie, L. Karkkainen, and K. Rummukainen, Nucl. Phys. **B333** (1990), 100.

[39] B. Beinlich, F. Karsch, and A. Peikert, Physics Letters B **390** (1997), no. 1-4, 268274.

[40] S. Huang, J. Potvin, C. Rebbi, and S. Sanielevici, Phys. Rev. **D42** (1990), 2864, [Erratum: Phys. Rev.D43,2056(1991)].

[41] T. Boeckel and J. Schaffner-Bielich, Phys. Rev. **D85** (2012), 103506, `arXiv:1105.0832` [astro-ph.CO].

[42] J. C. Miller and O. Pantano, Phys. Rev. D **42** (1990), 3334.

[43] J. I. Kapusta, A. P. Vischer, and R. Venugopalan, Phys. Rev. **C51** (1995), 901, `arXiv:nucl-th/9408029` [nucl-th].